International Journal of Peptide Research and Therapeutics (© 2007)
DOI: 10.1007/s10989-006-9058-8

Chimeric Protein Engineering

Jianwen A. Feng,[1] Lee A. Tessler[1] and Garland R. Marshall[1,2]

(Accepted November 17, 2006)

Protein stability can be enhanced by the incorporation of non-natural amino acids and semi-rigid peptidomimetics to lower the entropic penalty upon protein folding through preorganization. An example is the incorporation of aminoisobutyric acid (Aib, α-methylalanine) into proteins to restrict the Φ and Ψ backbone angles adjacent to Aib to those associated with helix formation. Reverse-turn analogs were introduced into the sequences of HIV protease and ribonuclease A that enhanced their stability and retained their native enzymatic activity. In this work, a chimeric protein, design_4, was engineered, *in silico*, by replacing the C-terminal helix of full sequence design protein (FSD-1) with a semi-rigid helix mimetic. Residues 1–16 of FSD-1 was ligated *in silico* with the N-terminus of a phenylbipyridyl-based helix mimetic to form design_4. The designed chimeric protein was stable and maintained the designed fold in a 100-nanosecond molecular dynamics simulation at 280 K. Its β-hairpin adopted conformations that formed three additional hydrogen bonds. Compared to FSD-1, design_4 contained fewer peptide bonds and internal degrees of freedom; it should, therefore, be more resistant to proteolytic degradation and denaturation.

KEY WORDS: protein engineering; helix mimetic; peptidomimetic; chimeric protein.

INTRODUCTION

Designing a protein sequence that folds into a designed three-dimensional shape is known as the inverse protein-folding problem. In nature, protein sequences are limited to combinations of the naturally occurring 20 amino acids and their post-translational modifications. Incorporation of non-natural amino acids and semi-rigid peptidomimetics provides unique possibilities for designing proteins that adopt a stable predetermined fold, allowing protein engineering to become a reality. Limiting segmental dynamics may be a useful probe of enzyme mechanism and/or specificity and also be of commercial interest in the production of super stable biocatalysts for green chemistry. For example, multiple tons of the proteolytic enzyme subtilisin, engineered to be stable in detergents at alkaline pH and elevated temperatures, are consumed annually in laundry detergents (Gupta et al., 2002). To be able to synthetically explore such topics is a direct outcome of the invention of solid-phase peptide chemistry and a stated objective (see discussion of work on ribonuclease A) of its inventor, R. Bruce Merrifield (Merrifield, 1993).

As the simplest example of preorganization, incorporation of aminoisobutyric acid (Aib, α-methylalanine) into proteins restricts the Φ and Ψ backbone angles adjacent to Aib to angles associated with helix formation (Marshall and Bosshard, 1972, Marshall et al., 1990). It is believed that Aib lowers the entropic penalty of helix formation upon protein folding due to

[1] Center for Computational Biology, Department of Biochemistry and Molecular Biophysics, Washington University, 700 S. Euclid Ave, St. Louis, MO, 63110, USA.
[2] Correspondence should be addressed to: Garland R. Marshall, Center for Computational Biology, Department of Biochemistry and Molecular Biophysics, Washington University, 700 S. Euclid Ave, St. Louis, MO, 63110, USA. Tel.: +1-314-362-1575; Fax: +1-314-747-3330; e-mail: garland@pcg.wustl.edu.

preorganization. By the same principle, incorporating semi-rigid mimetics of α-helices, β-sheets, and reverse turns into a protein would *minimize the entropy* lost on folding through preorganization, while retaining the interactive surface features that optimize the favorable *enthalpic interactions* in the folded state. The first examples include the incorporation of reverse-turn analogs into the enzymes HIV protease and ribonuclease A. Chimeric proteins should be thermodynamically more stable because their fold space is limited by semi-rigid mimetics that reduce the entropic penalty upon folding into the desired 3D structure. In addition, semi-rigid mimetics should promote the rate of protein folding by nucleation. Modular secondary structure mimetics can serve as building blocks in the design of ultra-stable, catalytically active chimeric proteins that resist proteolytic degradation and denaturation.

Computational protein design methods identify *de novo* amino acid sequences that can be folded into predefined topologies (Dahiyat and Mayo, 1997, Kuhlman et al., 2003). The 28-residue full sequence design (FSD-1) ββα protein was designed by Dahiyat and Mayo to form a stable zinc-finger ββα fold independent of zinc binding (Dahiyat and Mayo, 1997). Starting with the backbone coordinates of the zinc-finger protein Zif268, they selected side-chain rotamers to optimize side-chain/side-chain and backbone/side-chain interactions. The designed protein was synthesized and its structure solved by NMR; the resulting structure's overall backbone RMSD was 1.98 Å relative to the computationally designed target. Residues 3–12 were assigned as β-hairpin, and residues 15–26 were assigned as α-helical (Fig. 1). We selected FSD-1 as the template for chimeric protein engineering because its α-helix may be replaced with a semi-rigid helix mimetic, its stability was predicted by computational methods, and its short peptidic segment can be readily synthesized by solid-phase peptide synthesis and chemically ligated to the mimetic Experimental observations and theoretical calculations suggested that helical mimetics based on a terphenyl scaffold can correctly orient the i, $i + 3/i + 4$, and $i + 7$ side chains that formed one side of the surface of an α-helix (Yin et al., 2005a, b, Che et al., 2006). To further investigate the stabilities of helix mimetics, chimeric proteins have been designed, *in silico*, by ligating helix mimetics and the β-hairpin sub-domain of FSD-1. A 100-ns molecular dynamics (MD) simulation showed that one of these chimeric proteins was more stable than the native structure and maintains the expected fold during simulations.

MATERIAL AND METHODS

All FSD-1 simulations were carried out using GROMACS 3.3.1 running at the Texas Advanced Computing Center (TACC) (Van Der Spoel et al., 2005, Berendsen et al., 1995, Lindahl et al., 2001). Computational times on TACC were allocated as part of a TeraGrid Development Allocation award. The starting structure for the simulations was obtained from the PDB (ID: 1FSV). 1FSV is the restraint-minimized average structure of an ensemble of NMR structures (ID: 1FSD). The protein was solvated in a cubic box of 5661 TIP3P (Jorgensen et al., 1983) water molecules with at least 10 Å of solvent between any protein atom and the edge of the periodic box. The positively charged protein was neutralized with 5 molecules of chloride ions to form a charge-neutral system. Parameters were defined by the OPLSAA/L 2001 force field (Kaminski et al., 2001). Periodic boundary conditions were included. The constant pressure and temperature (NPT) ensemble was chosen and temperature and pressure (1 atm) were coupled using Berendsen's method (Berendsen et al., 1984). The initial solvated system was energy minimized, and heated by 50 K ncrements to the desired temperatures with each heating cycle lasting 20 ps. The production MD simulations were carried out with a time step of 2 fs. A linear constraint solver (LINCS) was applied to constrain hydrogen bond lengths (Hess et al., 1997). Long-range electrostatics were computed using particle mesh Ewald (PME) summation (Essmann et al., 1995). Snapshots were recorded every 20 ps.

Chimeric proteins were engineered, *in silico*, by ligating semi-rigid helix mimetics to residues 1–16 of 1FSV. Low energy conformations of mimetic 1 were generated by the Monte Carlo multiple minimum method in MacroModel. The number of Monte Carlo steps was 100,000, and the energy cutoff was 21.0 kJ/mol. The resulting conformers were superposed on the helical part of 1FSV by overlapping the Cα atoms of Leu18, Phe21 and Phe25 with the respective Cα atoms on the mimetic. Residues 17–28 of 1FSV were deleted and the conformation with the lowest RMSD was ligated to residues 1–16 via a peptide bond. The resulting chimeric protein was used as the starting model for molecular simulations. All implicit water dynamics simulations were carried out using MacroModel 9.1 (Schrodinger, 2006). The OPLS2005 force field parameters were used in these simulations. Solvent was treated implicitly with generalized Born/solvent-accessible surface area (GB/SA) approximation (Still et al., 1990). Structures were energy minimized and heated to the production temperature, 280 K, over 40 ps. SHAKE was applied to constrain hydrophobic hydrogen-bond lengths (Ryckaert et al., 1977). Total simulation time was 100 ns with a time step of 1.5 fs and snashots were recorded every 10 ps.

The GROMACS package provided analysis tools for calculating root mean square deviation (RMSD), root mean square fluctuation (RMSF), and radius of gyration for the explicit water FSD-1 simulations. GROMACS also included a cluster analysis tool. Unpublished scripts were used to calculate RMSD for the chimeric proteins. RMSD values were calculated over backbone atoms unless noted otherwise. Molecules were either visualized with Maestro or VMD (Humphrey et al., 1996, Schrodinger, 2006).

RESULTS AND DISCUSSION

Rigidifying helix mimetics to orient the interaction surface favoring recognition with its complementary

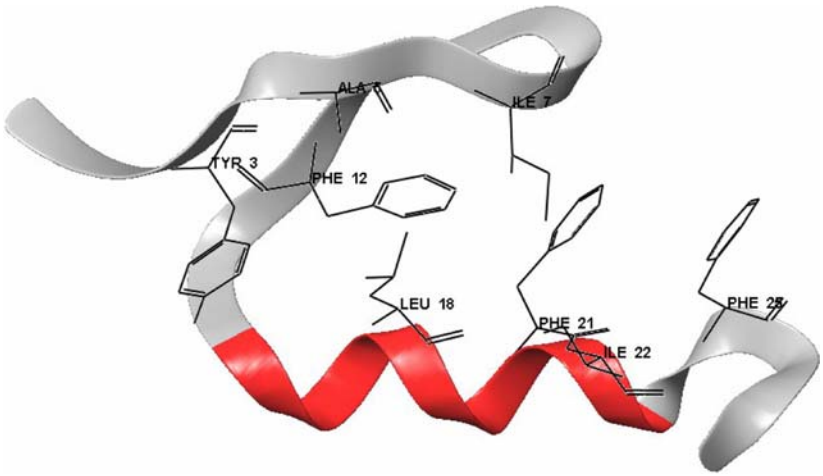

Fig. 1. Ribbon representation of FSD-1 with hydrophobic core residues displayed (PDB code 1FSV). Residues Leu18, Phe21 and Phe25 from the α-helix contribute to the stabilizing hydrophobic core. Residues 3–12 are assigned as a β-hairpin, and residues 15–26 are assigned as an α-helix.

protein surface is a ''double-edged sword''. It is very difficult, if not impossible, to find rigid scaffolds that overlap exactly the spatial orientation of C_α-C_β vectors and $\chi 1$ rotational angles of side chains while maintaining a high degree of scaffold rigidity. Introducing conformational constraints for secondary structure may prevent side chains from making optimal surface interactions to stabilize a fold. The impact of preorganization on energetics was first illustrated in a chimeric protein that incorporated an unusual bicyclic dipeptide reverse-turn analog (bicyclic turn dipeptide: BTD) into HIV protease. It showed an anticipated increase in fold stability, but of limited amount (Baca et al., 1993). The BTD HIV-1 protease was fully active, specific for native ligands, and more resistant to thermal inactivation. In another example of preorganization, Imperiali and co-workers used a D-proline residue to induce a type II′ β-turn centered about residues 4–5 of their BBA proteins (Struthers et al., 1996). Although they did not quantify the energetic contribution of incorporating such a rigid residue, it was essential for the folding of the proteins (Struthers et al., 1996, 1998).

Ribonuclease A

Ribonuclease A is a soluble 124-residue protein that catalyzes the endonucleolytic cleavage of nucleosides (Raines, 1998). A di-β-peptide, Nip-D-nip, was used to nucleate a β-hairpin at Asn113-Pro114 that enhanced stability without impacting enzymatic activity (Arnold et al., 2002). To investigate what was felt to be a minimal effect on the melting temperature ($\Delta T_m = 1.2 \pm 0.3$ °C), the crystal structure of RNAse was minimized, the turn mimetic Nip-D-nip inserted for Asn113-Pro114 and the chimeric structure reminimized. The two additional methylenes of the two β-amino acids were readily incorporated into the structure by simply extending the hairpin loop with nearly identical torsion angles of the rest of the peptide backbone (Fig. 2). Thus, no difference was found between the minimum-energy structures of the two structures suggesting that Nip-D-nip did not disrupt the extended β-sheet, and enthalpic stabilization should be maintained.

In order to evaluate the impact on the entropy of the two systems, an MD simulation of 100 ps was run at 300 K with GB/SA implicit water using MacroModel (Schrodinger, 2006). The metric selected for reverse-turn propensity was the distance between the α-carbons of residues 112 and 115. In native RNAse, the distance between the two α-carbons was less than 7 Å over 80% of the simulation; in the Nip-D-nip chimeric protein, the distance was less than 7 Å for only 10% of the time. While this difference does not directly estimate the amount of preorganization in the unfolded RNAse versus the chimeric protein, it does indicate that the introduction of two additional methylenes in the backbone of the loop by Nip-D-nip dramatically increases its inherent flexibility and compromises the impact of preorganization of the entropy of folding. In contrast, the use of the reverse-turn nucleators, Pro-D-pro or D-pro-Pro, enhanced the reverse-turn potential to that or greater than that

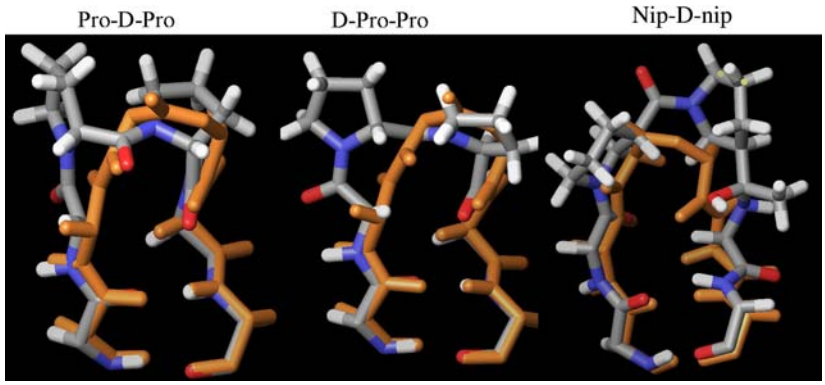

Fig. 2. Ribonuclease A β-hairpin (gold) and its turn mimetics.

of native Asn-113-Pro114 in accordance with previous estimates of reverse-turn nucleation by Takeuchi and Marshall (1998). From these results, one could predict that the thermal stability of a chimeric RNAse with either Pro-D-pro or D-pro-Pro replacing Asn113-Pro114 would be significantly greater than that of the chimeric RNAse with Nip-D-nip.

FSD-1

Helical structures represent one of the most common structural motifs and recognition sites in proteins. One face of an α-helix can be mimicked by a scaffold that correctly projects the side chains of residues *i*, *i* + *3*, *i* + *4*, and *i* + *7* (Fig. 3). The common surface formed by the *i*, *i* + *3*, *i* + *4*, and *i* + *7* residues of an α-helix is involved in molecular recognition. There are 3.6 residues per turn of the idealized α-helix, with an axial rise of 1.5 Å per residue. The characteristic axial rise between these residues is 4.5 Å (*i*, *i* + *3)* or 6.0 Å (*i*, *i* + *4)*. Helical peptides are stabilized by extensive, but weak intrachain H-bonds. A helix-mimetic scaffold developed by Che and Marshall can correctly place the Cα-Cβ vectors of the *i*, *i* + *3* and *i* + *7* residues within 0.314 Å RMSD of the ideal helix (Fig. 3) (Che et al., 2006). Axial rise between residues (*i*, *i* + *3)* and between residues (*i* + *3*, *i* + *7)* are within 0.3 Å, therefore; distances between side chains of the scaffold closely approximate the respective axial distances of natural helices. In FSD-1, residues Leu18 (*i*), Phe21 (*i* + *3*) and Phe25 (*i* + *7*) form one side of an alpha helix and make up part of the hydrophobic core (Fig. 1) and Phe21 and Phe25 were 80% buried. Visual inspection shows the *i* + *4* isoleucine residue (Ile22) also plays a role in forming the hydrophobic core, but it was not included in our mimetic design due to the anticipated increase in synthetic difficulty. In the designed chimeric proteins, the α-helical region of FSD-1 (PDB code: 1FSV) was replaced with designed helix mimetics to form chimeric proteins. Four slightly different helix mimetics were designed to increase the chance of presenting a hydrophobic surface that forms favorable interactions with the β-hairpin to stabilize a chimeric protein (Fig. 4). Mimetic 1 contained a hydroxyl group that could form intramolecular H-bonds. Mimetic 2 lacked a methyl group on ring C which increased its conformational flexibility by removing steric interactions with ring B. In mimetic 3, nitrogens on the pyridine rings are placed in the *para* position in relation to the side chains. Mimetic 4 is similar to mimetic 1 with the exception

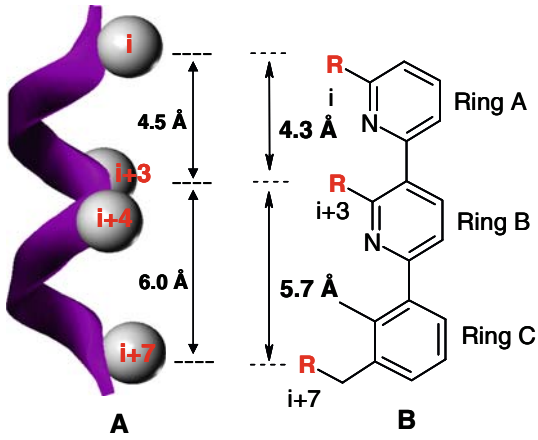

Fig. 3. (A) Idealized α-helix geometry with 4.5 Å rise between residues *i* and *i* + 3 and 6.0 Å rise between residues *i* and *i* + 4. These residues are located on the same face of the helix. (B) A pheylbipyridyl helix mimetic scaffold that captures the helix axial rise in distances.

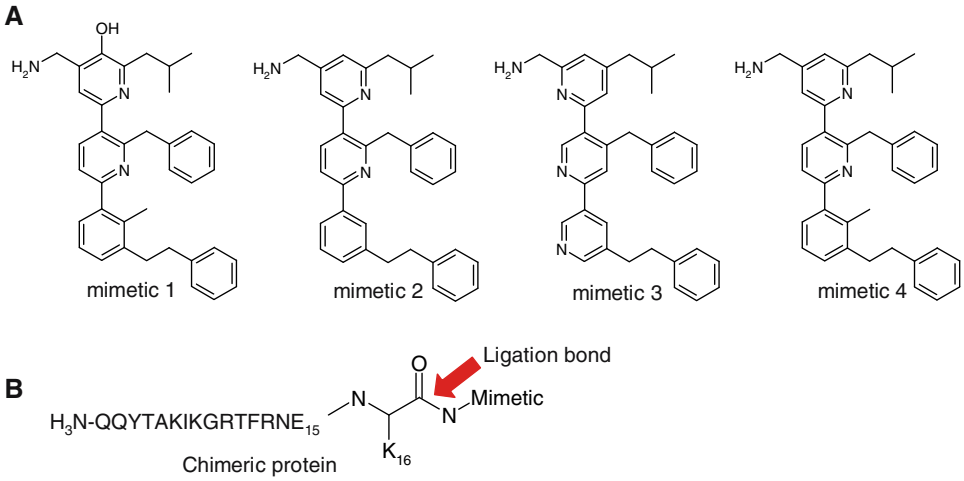

Fig. 4. (A) Four mimetics were designed to mimic the surface formed by residues Leu18, Phe21 and Phe25 of FSD-1. (B) A peptide bond ligated the first 16 residues of FSD-1 to a helix mimetic to form a chimeric protein. Four chimeric proteins were designed, each containing a different mimetic.

of the hydroxyl group. Side chains were attached to the mimetic scaffold to represent residues Leu18, Phe21, and Phe25. The hydrophobic surface formed by the side-chains of the mimetics was expected to be similar to that of the native helix.

FSD-1 Dynamics

MD simulations can be used to analyze the folding and unfolding of proteins (Snow et al., 2002, Lei et al., 2006, Jang et al., 2006, Lei and Duan, 2004). Duan et al. performed multiple 10 ns simulations in explicit solvent at different temperatures to study the roles of plastic β-hairpin and weak hydrophobic core in the stability and unfolding of FSD-1 (Lei and Duan, 2004). Pak and co-workers simulated FSD-1, BBA5 and 1PSV in implicit solvent to study the free energy surfaces of mini-proteins (Jang et al., 2006). These mini-proteins are attractive for computational studies due to their small size that allows for longer time-scale simulations. Pande and co-workers observed folding events in tens of thousands of ns (700 ms) simulations of a BBA5 double mutant via their Folding@Home project (Snow et al., 2002). For this study, 105 ns MD simulations were performed at 280, 300, 330 and 360 K to study the thermal stability of FSD-1. These simulation temperatures were chosen to match the NMR experimental temperature of FSD-1 at 280 K and to study the stability of FSD-1 near its melting temperature of 315 K (Dahiyat and Mayo, 1997).

RMSD from the starting structure, 1FSV, were calculated over backbone coordinates for the four MD trajectories (Fig. 5). At 280 K, the MD trajectory stabilized after 2 ns with an average RMSD of 3.0 Å. Cluster analysis resulted in every structure being placed in the same cluster with an average backbone RMSD of 1.43 Å from the mean structure. The pair-wise backbone RMSD ranged from 0.29 to 5.38 Å, with the mean at 1.89 Å. The 41 NMR conformations of FSD-1 contained two hydrogen bonds between residue Tyr3 in β-strand one and Phe12 in β-strand two (Table I). No additional hydrogen bonds were found between residues in β-strand one (3–6) and residues in β-strand two (9–12). Hydrogen bonds were defined by a maximum donor-acceptor distance of 3.0 Å and a minimum donor-acceptor angle of 90°. In the 280 K simulation, the two hydrogen bonds between Tyr3 and Phe12 were formed 50.7% of the time, and at least one of the two hydrogen bonds were formed 92.0% of the time. A third inter-strand hydrogen bond was formed less than 1% of the time when residues 3–6 and 9–12 were included in the calculation. The two hydrogen bonds between Tyr3 and Phe12 were essential in stabilizing the β-hairpin. At 300 K, the RMSD was similar to that at 280 K for the initial 15 ns, and then continually increased to over 4 Å. At 50 ns, the RMSD value jumped from ~3.0 Å to ~4.0 Å. After 50 ns, the RMSD values ranged from 3.0 to 5.5 Å and the two hydrogen bonds between Tyr3 and Phe12 were formed only 10.7% of the time. The β-hairpin secondary structure

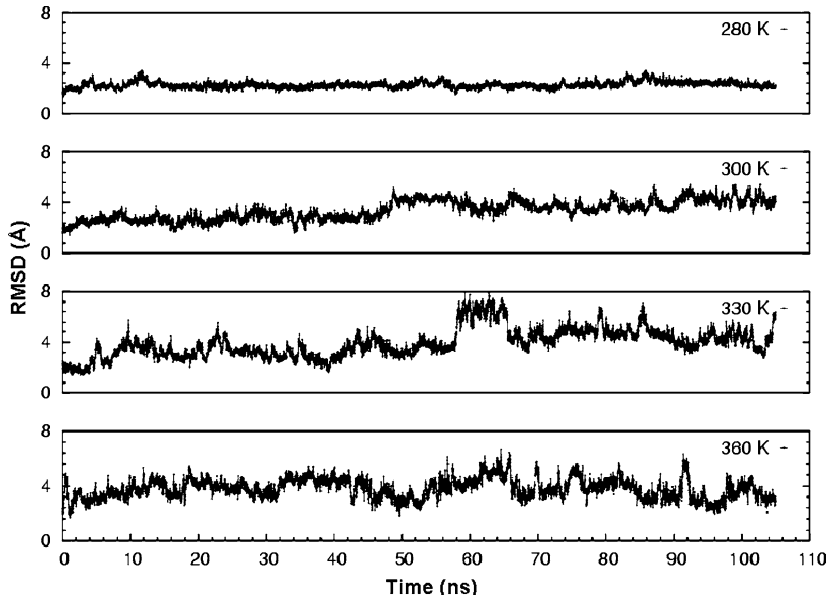

Fig. 5. RMSDs from the starting structure (PDB code 1FSV) were calculated over backbone coordinates for four MD trajectories at the respective temperatures.

was fluctuating between the folded and unfolded states. At 330 K, FSD-1 began to unfold at 58 ns, and the RMSD from native reached 8.33 Å at time point 59.24 ns (Fig. 5). At time point 59.24 ns, the hydrophobic core between the α-helix and the β-hairpin was lost. In addition, the α-helix was partially unfolded and the β-hairpin was completely lost (Fig. 6). After the 65 ns time point, FSD-1 sampled transitions between the folded and unfolded states. At time point 103.2 ns, FSD-1 refolded and the RMSD value was 3.08 Å. The 300 K simulations sampled both folded and unfolded states of FSD-1. At 360 K, the RMSD plot is similar to that at 330 K, but the largest RMSD value was 6.69 Å. The lowest RMSD value after the 60 ns time point was 1.97 Å at 96.04 ns. The absolute deviation in the 360 K simulation was lower compared to the 330 K simulation even though the former was at a higher temperature. The average RMSD for the 330 and 360 K simulations were 3.93 and 3.80 Å, respectively. This indicates that the simulations only captured a snapshot of the energy landscape even though 100 ns simulations were longer than most MD simulations.

RMSF plot showed that protein motion or fluctuation was highest at 330 K (Fig. 7). The termini were most flexible and in good agreement with NMR experimental data (Dahiyat and Mayo, 1997). Of the non-termini residues, residues 7–9 which are turn residues within the β-hairpin showed the most flexibility. This observation is consistent with those of Duan et al. (Lei and Duan, 2004). At 330 K, the RMSF value for residue 8 is 4.23 Å. The β-hairpin is slightly more stable than the turn residues, while the α-helical region was the most stable. Radius of gyration, $g(r)$, plots for the protein heavy atoms at different temperatures is shown in Fig. 8. The $g(r)$ for the native protein at 280 K ranged from 9 to 10 Å. The largest $g(r)$, 12.25 Å, was observed in the 330 K simulation at time point 62.7 ns. Figure 9 shows that $g(r)$ values for some unfolded states are similar to that of the folded protein. This indicates that the folded and some unfolded states are similarly compact; therefore, $g(r)$ per se is a necessary, but not sufficient requirement, for a native-folded structure.

Table I. Percentage of conformers that formed β-hairpin H-bonds

	Tyr3–Phe12	Ala5–Lys8	Ala5–Gly9	Ala5–Arg10
FSD-1 NMR	100% (2)	–	–	–
FSD-1 280 K	50.7%[a] (2)	–	–	–
Design_4 280 K	95.4%(2)	97.1% (1)	97.5% (1)	97.3% (1)

Numbers inside the ( ) indicates number of hydrogen bonds formed.
[a]FSD-1 280° K formed one H-bond in 92.0.7% of the conformations.
–: Indicates that H-bond was not observed for the specified residues.

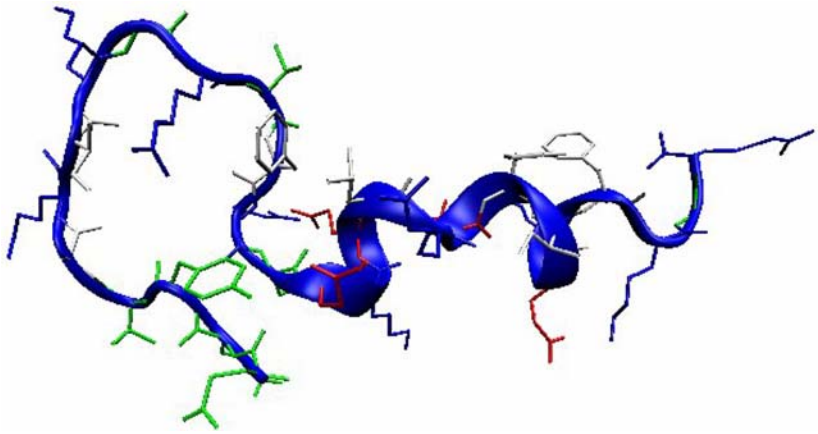

Fig. 6. Structure of FSD-1 at time point 59.24 ns. The simulation temperature was 330 K. The hydrophobic core was disrupted and the β-hairpin was completely unfolded. The α-helix was partially unfolded. The backbone RMSD from native structure was 8.33 Å.

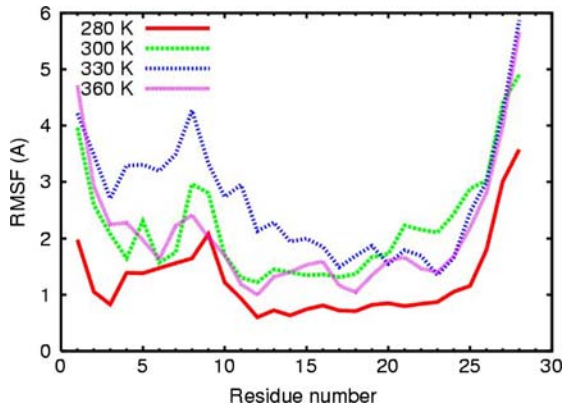

Fig. 7. C-α carbon RMSF values for the four MD trajectories of FSD-1.

Chimeric Protein Dynamics

MD simulations of native FSD-1 provided a baseline for understanding the stability of this protein at different temperatures. Comparing MD trajectories at 280 K of FSD-1 derived chimeric proteins to those of FSD-1 provided insight into the relative stabilities of the chimeras. Four designed chimeric proteins were simulated using the MacroModel molecular modeling package (Schrodinger, 2006). These simulations were done in implicit solvent as a first approximation to explicit solvent simulations. This route was chosen because force field parameters were readily assigned using the graphical user interface, Maestro. In addition, using an implicit solvent method reduced the computational time by a significant amount. To verify the accuracy of the force field parameters for the scaffold atoms, torsional energy scans were performed on representative small molecules using both quantum and molecular mechanics methods (Kaminski et al., 2001). The results show that molecular mechanics parameters gave good agreement with quantum mechanical torsional profiles (unpublished data).

Chimeric proteins were created, *in silico*, by replacing residues 17 to 29 of FSD-1 with a helical peptidomimetics. A peptide bond ligated the C-terminus of Lys16 to the "amino terminus" of the mimetic. Of the four designed chimeric proteins, three unfolded during the 100 ns simulations at 280 K, and their RMSD between 80 and 100 ns were greater than or equal to 6 Å. Design_4, which ligated mimetic 4 with residues 1–16 of FSD-1, remained stable throughout the 100 ns simulation (Fig. 10). RMSD from the starting structure shows that design_4 stabilized after 5 ns with an average heavy atom RMSD value of ~4 Å. Figure 10 shows a superposition of the staring structure with a representative structure from the trajectory in which the heavy atom RMSD was 3.81 Å. At time point 3.3 ns, the peptidomimetic segment separated from the β-hairpin and moved into solvent and its heavy atom RMSD was 5.28 Å. It refolded quickly into a more favorable orientation at time point 3.5 ns and wiggled in position throughout the simulations. The backbone RMSD of the β-hairpin (residues 3–12) was 2.23 Å indicating that the β-hairpin was folded. It was shown in the 280 K FSD-1 simulation that hydrogen bonds

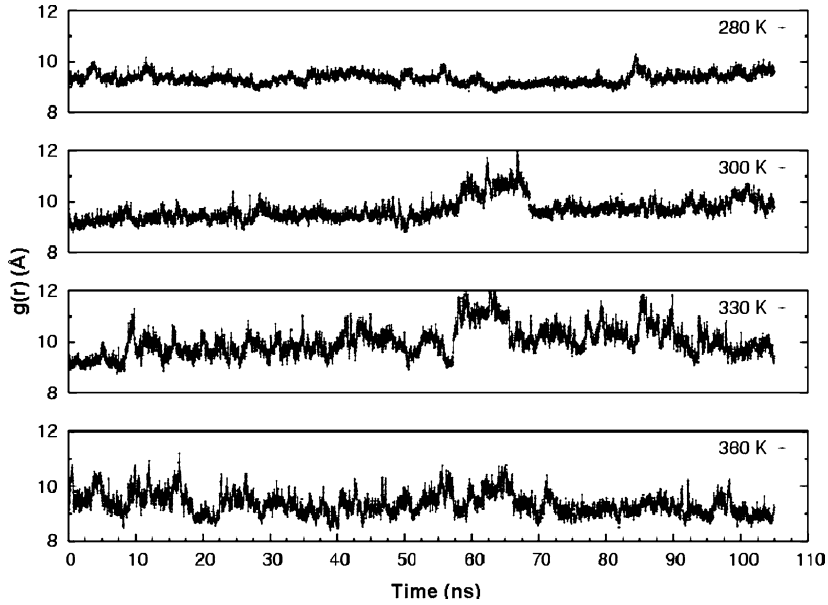

Fig. 8. Radius of gyration, $g(r)$, plots in angstroms for the four 1FSV MD trajectories at the respective temperatures.

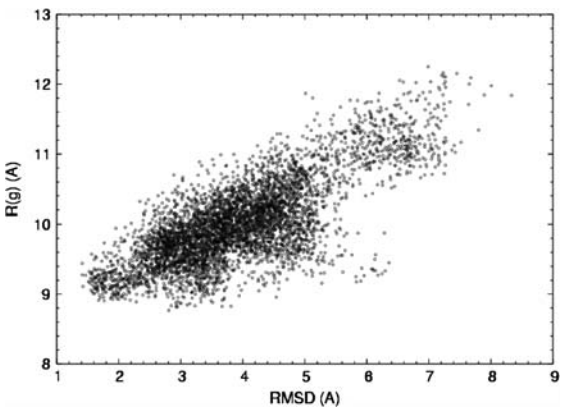

Fig. 9. Radius of gyration plot for FSD-1 at 330 K. The compactness of some unfolded states was similar to that of the folded state.

between Tyr3 and Phe12 were important indicators of β-hairpin formation. In the design_4 chimeric protein, the two hydrogen bonds between Tyr3 and Phe12 were initially absent, but they formed after 2 ns and was 95.4% formed throughout the 100 ns simulation (Table I). Additional hydrogen bonds were formed between Ala5 in β-strand one and residues Lys8, Gly9 or Arg10 in β-strand two to further stabilize the β-hairpin. Between residues Ala5 and Lys8, 97.1% of conformations formed one H-bond; 97.5% of conformations formed one H-bond between Ala5 and Gly9; 97.3% of conformations formed one H-bond between Ala5 and Arg10; and 21.5% formed two H-bonds. These additional H-bonds nucleated β-hairpin formation and enhanced its stability as compared to the more flexible β-hairpin in FSD-1. The backbone RMSD for residues 3–12 between a representative design_4 conformer and 1FSV was 1.85 Å indicating that they adopted similar conformations. The amino acid sequence was identical for both hairpin segments, but their interactions with the helical region were different.

The helix mimetics were ligated to the β-hairpin via Lys16. For the chimeric proteins to fold similar to FSD-1, the backbone torsion angles of Lys16 in the chimeric protein should be similar to that of FSD-1. To compare the backbone conformations of this residue, we measured Lys16 Φ and Ψ angles of FSD-1 and those of chimeric design_4 (Fig. 11). Both simulations were performed at 280 K. While Lys16 in both proteins occupied the α-helix region of the Ramachandran plot, the Lys16 Φ and Ψ angles of FSD-1 and design_4 ranged from −180° to 0° and from −60° to −120°, respectively. The angles were from −60° to 30° for FSD-1 and from −60° to 0° for design_4. Allowed Φ and Ψ regions for Lys16 in design_4 were smaller than that of FSD-1. The Lys16 in FSD-1 was more flexible than its counterpart in design_4 suggesting the chimeric protein maybe more rigid.

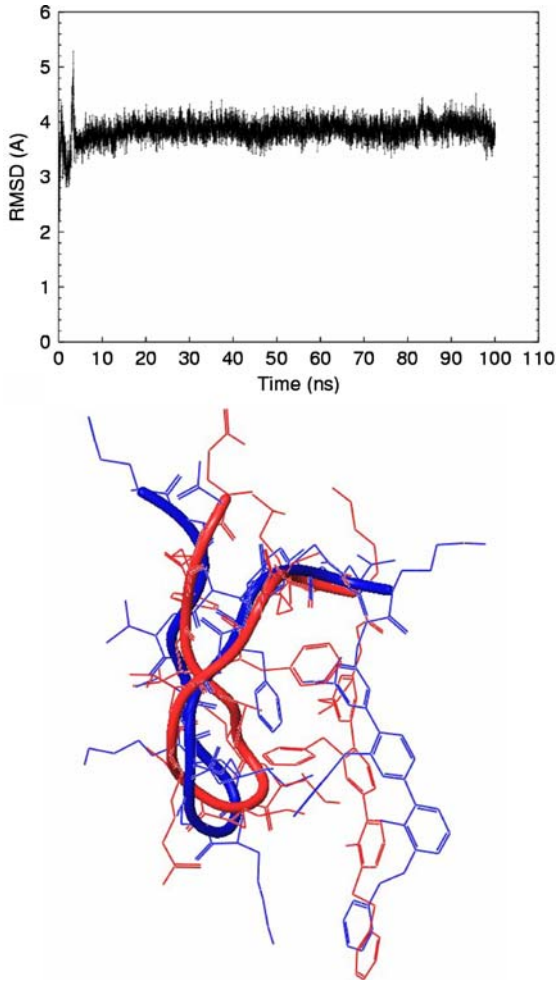

Fig. 10. Top: Heavy atom RMSD plot chimeric protein design_4 shows that it stayed folded throughout the 100 ns dynamics simulation at 280 K. Bottom: Superposition of the starting structure (orange) with a representative structure (blue) from the MD trajectory. The heavy atom RMSD was 3.81 Å. The backbone RMSD of the β-hairpin (residues 3–12) was 2.23 Å.

CONCLUSION

MD simulations showed that one of the four chimeric proteins was more stable at 280 K and its fold was similar to that of FSD-1. The β-hairpin in design_4 formed more hydrogen bonds compared to FSD-1 which suggested that design_4 maybe more stable. In addition, replacing helical residues 17–28 of FSD-1 appeared to make residue Lys16 in design_4 more rigid. In the MD simulation, residues 7–9 of FSD-1 exhibited the highest flexibility. Incorporation of semi-rigid turn mimetics like Pro-D-pro and D-pro-Pro may further enhance the stability of a chimeric FSD-1 protein. In stabilizing the folded state with semi-rigid mimetics, we also destabilize the unfolded states by eliminating a percentage of the unfolded space, thereby reducing the entropic cost of folding.

A protein that stays folded during a 100 ns simulation indicated that this conformation occupies an energy minimum. Longer simulation time and/or higher temperatures may result in the unfolding of design_4. Nevertheless, these preliminary results showed the feasibility of designing chimeric proteins that contain both natural amino acid residues and a helical peptidomimetic as a means of enhancing stability. It is worth nothing that FSD-1 simulations were performed in explicit solvent, and the chimeric protein simulations have only been performed in implicit solvent at this time. Further simulations of design_4 in explicit solvent and at different temperatures using GROMACS are planned. Replica exchange molecular dynamics (REMD) will be employed to enhance sampling (Sugita and Okamoto, 1999; Jang et al., 2006). While this manuscript was in preparation, Duan and co-workers published data on five 200-ns simulations of FSD-1 at 300 K (Lei et al.,

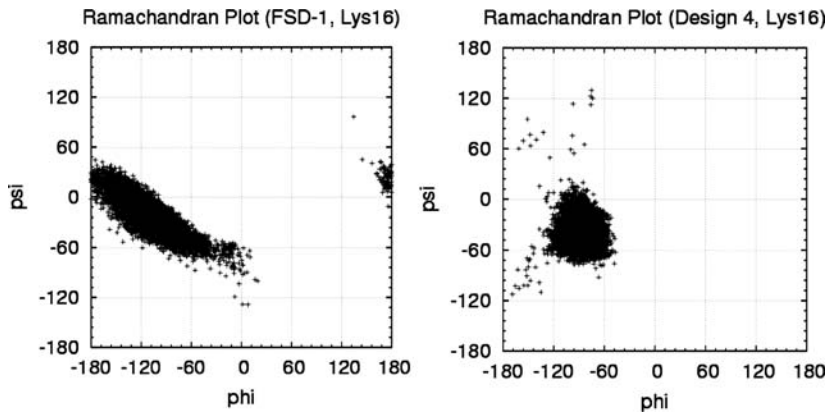

Fig. 11. Ramachandran plots for residue Lys16 of FSD-1 (left) and design_4 (right). The simulation temperatures were 280 K.

2006). The additional information contained will provide useful comparisons with data collected from design_4 simulation.

ACKNOWLEDGMENTS

The authors would like to thank Daniel J. Kuster and Christy Taylor, Ph.D. for valuable discussions and critical reading of this manuscript. This research was supported in part by NIH research grant (GM 08460) to GRM. J.F. also acknowledges graduate support from the Division of Biology and Biomedical Science of Washington University in St. Louis, the Computational Biology Training Grant (GM 008802), and the Kauffman Foundation. Computational resources were supported in part by TeraGrid.

REFERENCES

Arnold, U., Hinderaker, M. P., Nilsson, B. L., Huck, B. R., Gellman, S. H. and Raines, R. T.: 2002, *J. Am. Chem. Soc.* 124, 8522–8523.

Baca, M., Alewood, P. F. and Kent, S. B.: 1993, *Protein Sci.* 2, 1085–1091.

Berendsen, H. J., Postma, J., Dinola, A. and Haak, J.: 1984, *J. Phys. Chem.* 81, 3684–3690.

Berendsen, H. J. C., Vanderspoel, D. and Vandrunen, R.: 1995, *Comput. Phys. Commun.* 91, 43–56.

Che, Y., Brooks, B. R. and Marshall, G. R.: 2006, *J. Comput. Aided Mol. Des.* 20, 109–130.

Dahiyat, B. I. and Mayo, S. L.: 1997, *Science* 278, 82–87.

Essmann, U., Perera, L., Berkowitz, M. L., Darden, T., Lee, H. and Pedersen, L. G.: 1995, *J. Chem. Phys.* 103, 8577–8593.

Gupta, R., Beg, Q. K. and Lorenz, P.: 2002, *Appl. Microbiol. Biotechnol.* 59, 15–32.

Hess, B., Bekker, H., Berendsen, H. J. C. and Fraaije, J. G. E. M.: 1997, *J. Comput. Chem.* 18, 1463–1472.

Humphrey, W., Dalke, A. and Schulten, K.: 1996, *J. Mol. Graph.* 14, 33 .

Jang, S., Kim, E. and Pak, Y: 2006, *Proteins* 62, 663–671.

Jorgensen, W. L., Chandrasekhar, J., Madura, J. D., Impey, R. W. and Klein, M. L.: 1983, *J. Chem. Phys.* 79, 926–935.

Kaminski, G. A., Friesner, R. A., Tirado-Rives, J. and Jorgensen, W. L.: 2001, *J. Phys. Chem. B* 105, 6474–6487.

Kuhlman, B., Dantas, G., Ireton, G. C., Varani, G., Stoddard, B. L. and Baker, D.: 2003, *Sci.* 302, 1364–1368.

Lei, H., Dastidar, S. G. and Duan, Y.: 2006, *J. Phys. Chem. B Condens. Matter. Mater. Surf. Interfaces Biophys.* 110, 22001–22008.

Lei, H. and Duan, Y.: 2004, *J. Chem. Phys.* 121, 12104–12111.

Lindahl, E., Hessv, B. and van der Spoel, D.: 2001, *J. Mol. Model.* 7, 306–317.

Marshall, G. R. and Bosshard, H. E.: 1972, *Circ. Res.* 31(Suppl 2), 143–150.

Marshall, G. R., Hodgkin, E. E., Langs, D. A., Smith, G. D., Zabrocki, J. and Leplawy, M. T.: 1990, *Proc. Natl. Acad. Sci. USA* 87, 487–491.

Merrifield, B.: 1993, *Life During a Golden Age of Peptide Chemistry: The Concept and Development of Solid-phase Peptide Synthesis*, pp. , American Chemical Society, Washington, DC.

Raines, R. T.: 1998, *Chem. Rev.* 98, 1045–1066.

Ryckaert, J., Ciccotti, G. and Berendsen, H. J.: 1977, *J. Comput. Phys.* 23, 327 .

Schrodinger: 2006, Portland, OR 97021.

Snow, C. D., Nguyen, H., Pande, V. S. and Gruebele, M.: 2002, *Nature* 420, 102–106.

Still, W. C., Tempczyk, A., Hawley, R. C. and Hendrickson, T.: 1990, *J. Am. Chem. Soc.* 112, 6127–6129.

Struthers, M., Ottesen, J. J. and Imperiali, B.: 1998, *Fold Des.* 3, 95–103.

Struthers, M. D., Cheng, R. P. and Imperiali, B.: 1996, *Science* 271, 342–345.

Sugita, Y. and Okamoto, Y.: 1999, *Chem. Phys. Lett.* 314, 141–151.

Takeuchi, Y. and Marshall, G. R.: 1998, *J. Am. Chem. Soc.* 120, 5363–5372.

Van Der Spoel, D., Lindahl, E., Hess, B., Groenhof, G., Mark, A. E. and Berendsen, H. J.: 2005, *J. Comput. Chem.* 26, 1701–1718.

Yin, H., Lee, G. I., Park, H. S., Payne, G. A., Rodriguez, J. M., Sebti, S. M. and Hamilton, A. D.: 2005a, *Angew. Chem. Int. Ed. Engl.* 44, 2704–2707.

Yin, H., Lee, G. I., Sedey, K. A., Kutzki, O., Park, H. S., Orner, B. P., Ernst, J. T., Wang, H. G., Sebti, S. M. and Hamilton, A. D.: 2005b, *J. Am. Chem. Soc.* 127, 10191–10196.